

ONSET OF CONVECTION IN A MELTED ICE LAYER BETWEEN VERTICAL PLATES

M. A. HASSAB and M. M. SOROUR

Alexandria University, Faculty of Engineering, Mechanical Power Engineering,
Alexandria, Egypt

(Received 24 February 1981 and in revised form 1 October 1981)

Abstract—The stability of the conduction regime of natural convection in a vertical melted ice layer initially assumed to be at its melting temperature is studied using the linear theory. The stability curves, $Gr_c = Gr_c(T_1)$ and $h_c = h_c(T_1)$, show that the critical Grashof number Gr_c and the critical melting thickness h_c are dependent upon the stepped wall temperature T_1 , such that as T_1 is increased the change in heat transfer mode from conduction to convection is enhanced for all values of T_1 in the range of 1–30°C. Furthermore, it is found that the instability sets in as vertical travelling waves, with the secondary flow occurring as two-column waves for $T_1 < 7.1^\circ\text{C}$ and $T_1 > 9.4^\circ\text{C}$, and as three-column waves for $7.1^\circ\text{C} < T_1 < 9.4^\circ\text{C}$.

NOMENCLATURE

a ,	wave number;
C_p ,	specific heat;
C_i ,	c_i/U_0 , non-dimensional wave speed;
c_b ,	wave speed;
C_r ,	amplification factor;
D ,	$\partial/\partial Y$, operator;
g ,	gravity;
Gr ,	$= g \lambda_1 T_1^2 h^3/v^2$, Grashof number;
\tilde{Gr} ,	$= g \beta_0 T_1 h^3/v^2$, modified Grashof number;
h ,	$= 2S\sqrt{at}$, thickness of water layer;
L_f ,	heat of fusion;
k ,	thermal conductivity;
P ,	pressure;
Pr ,	$= v/\alpha$, Prandtl number;
S ,	$= h dh/2\alpha dt$, parameter;
St_w ,	$= C_p T_1/h_s$, Stefan number;
T ,	temperature;
T_1 ,	temperature of the heated wall;
t ,	time;
U_0 ,	$= g \lambda_1 T_1^2 h^2/v$, characteristic thermal velocity;
U, V ,	velocity components;
X, Y ,	$= (x, y)/h(t)$, non-dimensional coordinates;
x, y ,	coordinates with y measured normal to the water layer and x parallel to it.

Greek symbols

α, v	thermal diffusivity and kinematic viscosity;
ρ ,	density of the fluid.
θ ,	$= T/T_1$, dimensionless temperature;
ψ ,	$= U_0 h/v$, dimensionless stream function;
β_0 ,	coefficient of thermal expansion at the interface (absolute value);
β ,	$= \int_0^{T_1} -\frac{1}{\rho_0} \frac{d\rho}{dT} dT$, average coefficient of thermal expansion;
τ ,	$= \int v dt/h^2$, dimensionless time.

Superscripts

$\bar{}$,	mean quantities;
\prime ,	perturbed quantities.

INTRODUCTION

THE PURPOSE of this study is to gain insight into the process of melting. Attention is focused on the interaction between the thermal convection currents in the liquid and the formation of liquid at the instant melting begins. Ice layers in general are subjected to inevitable heat sources, thus temperature differences appear and heat is transferred by conduction and convection. Where as the effect of conduction can be easily described the convection process still yields some unsolved problems, due to the complex governing equations of the stability problems involved and the density anomaly of water [1].

The stability of the conduction regime of natural convection of common fluids in a vertical slot has been investigated in the past. Starting with the work of Gershuni [2] that limited for fluids having small Prandtl number, Rudakov [3] obtained results for Prandtl numbers up to 10 and found the instability to set as stationary convection at a Grashof number of about $Gr_c = 7700$. This result was experimentally confirmed by Vest and Arpac [4]. On the other hand, for very large Prandtl numbers Gill and Kirkham [5] found the instability to set in as travelling waves with $Gr_c = 9.4 \times 10^3 Pr^{-1/2}$. Korpella *et al.* [6] confirmed the results of the above investigators and covered a wide range of Prandtl numbers and showed a limiting value of $Pr = 12.7$ for the transition from stationary cells to travelling waves in the vertical direction.

In all these earlier studies, it is assumed that the temperature gradient is constant and the density is a linear function of temperature. However, these approximations do not apply accurately for a melting layer of ice, because the water density near 4°C is no longer linear with the temperature. In reviewing the literature

on the stability of melting ice, it was found that the published results are only restricted for the horizontal case under different dynamic and thermal boundary conditions [7-13].

These results indicate that the onset of free convection expressed by the critical Rayleigh number is not a single value but varies with temperature of the heated wall. Therefore, the present investigation is devoted to study the stability criteria of vertical melted ice layer confined inside a slender slot and subjected to a temperature difference varying from 0 to 30°C.

ANALYSIS

A Stefan problem which deals with the melting of an ice layer that is confined inside a vertical slender slot is considered as shown in Fig. 1. Initially the ice layer is assumed to be at its melting temperature $T = 0^\circ\text{C}$. At time $t = 0$, heating is initiated at one of the side walls by a step increase in the wall temperature to a constant value T_1 . As a result of heating a melt layer is formed as solid ice is transformed into water. For small thickness of the water layer, the heat is transferred only by conduction (except at the ends of the slot). Consequently, a laminar parallel flow will be developed as a result of the density difference in the fluid. As this thickness is gradually increased with time, the initial laminar motion breaks up and secondary flow appears in the form of either stationary horizontal cells or travelling waves. In this study, the conditions marking the onset of this secondary flow in the formed water layer, where the density anomaly can not be neglected, are investigated analytically as described below.

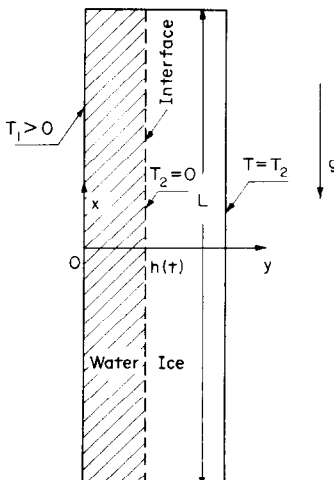


FIG. 1.

The base flow

Subject to the usual Oberbeck-Boussinesq approximation, the governing equations of motion and energy for the conduction regime of the natural laminar flow may be given as:

$$\frac{\partial \bar{u}}{\partial t} = \frac{1}{\rho_0} \frac{\partial \bar{P}}{\partial x} + v \frac{\partial^2 \bar{u}}{\partial y^2} - \frac{\bar{\rho}}{\rho_0} g, \quad (1)$$

$$\frac{\partial \bar{T}}{\partial t} = \alpha \frac{\partial^2 \bar{T}}{\partial y^2} \quad (2)$$

with the boundary conditions at $t \geq 0$,

$$\bar{u} = 0 \quad \text{at} \quad y = 0, h(t), \quad (3)$$

$$\bar{T} = T_1 \quad \text{at} \quad y = 0, \quad (3)$$

$$\bar{T} = 0 \quad \text{at} \quad y = h(t), \quad (3)$$

$$-K \frac{\partial \bar{T}}{\partial y} = \rho_0 L_f \frac{dh}{dt} \quad \text{at} \quad y = h(t), \quad (3)$$

and a mass balance for the closed system

$$\int_0^h \bar{u} dy = 0. \quad (4)$$

Here for the base flow, \bar{u} is the velocity in the vertical direction (i.e. x -direction), \bar{P} and \bar{T} are the pressure and temperature respectively, $\bar{\rho}$ is the density, and h is the thickness of the melted layer which is a function of time (see Nomenclature).

The density-temperature relationship for water within the temperature ranges concerned is assumed to be [14]:

$$\rho = \rho_m [1 - \lambda_1 (T - T_m)^2 - \lambda_2 (T - T_m)^3] \quad (5)$$

where ρ_m is the maximum density of water that occurs at $T_m = 4^\circ\text{C}$, $\lambda_1 = 0.793953 \times 10^{-5} \text{ }^\circ\text{C}^{-2}$ and $\lambda_2 = -0.6559 \times 10^{-7} \text{ }^\circ\text{C}^{-3}$. Before proceeding further, the similarity transformation is applied on equations (1) and (2) to transform the independent variables (t, y) into a new dimensionless variable $Y = y/h(t)$. With $U_0 = g\lambda_1 T_1^2 h^2/v$ as the thermal characteristic velocity, T_1 as reference temperature, and $P_0 = g\rho_0\lambda_1 T_1^2 h$ as a scale for pressure, one obtains:

$$D^2 \bar{U} + \frac{2S^2}{Pr} (Y D \bar{U} - 2\bar{U}) = F - (A_0 + \bar{\theta})^2 - l(A_0 + \bar{\theta})^3, \quad (6)$$

$$D^2 \bar{\theta} + 2S^2 Y D \bar{\theta} = 0, \quad (7)$$

$$\bar{U}(0) = \bar{U}(1) = 0, \quad (8)$$

$$\bar{\theta}(0) = 1, \quad \bar{\theta}(1) = 0, \quad (9)$$

$$D\bar{\theta}(1) = -2S^2/St_w$$

and

$$\int_0^1 \bar{U} dY = 0.$$

In these equations, $F = -(dP/dX) + (\rho_0 gh/P_0)$, $A_0 = -T_m/T_1$, $l = \lambda_2 T_1/\lambda_1$; see also the Nomenclature. In the above equations, the quantities subscripted by '0'

are chosen equal to those with subscript 'm'.

For the range of the stepped wall temperature T_1 considered in this study, the Stefan number St_w is of the order of 10^{-1} . The order of which suggests that the parameter S^2 related to it by equation (8) is of the same order (i.e. $S^2 \approx \frac{1}{2}St_w$) [15]. In addition from the relation between h and S^2 given above, it can be shown that the melting rate of ice expressed by the interfacial velocity, V_i , is of the order of 10^{-3} cm/s for a value of $h \approx 1$ cm. This velocity is extremely small compared to the thermal characteristic velocity U_0 ($\approx 10^2$ cm/s) thus its influence on the fluid motion is invisible. Furthermore, the effect of the void space created as a result of volume shrinkage (9%) during the phase transition from ice to water is also negligible since the shrinkage rate at the interface is about 9% of the magnitude of V_i .

Therefore, equations (4)–(9) could be simplified further by disregarding the terms containing the parameter S^2 . In doing so, the resultant equations can be solved analytically for $\bar{\theta}$ and \bar{U} respectively. Their solutions are given as:

$$\bar{U} = a_1 + a_2 Y^* + \frac{FY^{*2}}{2} - \frac{Y^{*4}}{12} - \frac{Y^{*5}}{20}, \quad (10)$$

$$\bar{\theta} = 1 - Y,$$

where

$$Y^* = \left(\frac{T_1 - T_m}{T_1} \right) - Y. \quad (11)$$

The coefficients a_1 , a_2 and F are to be obtained by letting the solution (10) for \bar{U} satisfy its boundary conditions (8) and (9). These expressions are quite lengthy and are omitted here.

The stability equations

To derive the perturbation equations needed for the analysis of stability which occurs as two-dimensional transverse waves [4], small quantities on the velocity components, pressure and temperature are defined as:

$$U = \bar{U}(Y) + U', \quad V = V',$$

$$P = \bar{P}(X) + P', \quad T = \bar{T}(Y) + T'. \quad (12)$$

Introducing these variables into the conservation equations of mass, momentum and energy, neglecting the non-linear terms, the following system of linear perturbations is obtained in the dimensionless form as:

$$\frac{\partial \bar{U}}{\partial X} + D\bar{V} = 0, \quad (13)$$

$$\frac{\partial \bar{U}}{\partial \tau} + Gr \bar{U} \frac{\partial \bar{U}}{\partial X} + Gr D\bar{U}\bar{V} = -\frac{\partial \bar{P}}{\partial X} + \nabla^2 \bar{U} + f\bar{\theta}$$

$$+ \frac{2S^2}{Pr} \left(X \frac{\partial \bar{U}}{\partial X} + YD\bar{U} - 2\bar{U} \right), \quad (14)$$

$$\frac{\partial \bar{V}}{\partial \tau} + Gr \bar{U} \frac{\partial \bar{V}}{\partial X} = -D\bar{P} + \nabla^2 \bar{V}$$

$$+ \frac{2S^2}{Pr} \left(X \frac{\partial \bar{V}}{\partial X} + YD\bar{V} - 2\bar{V} \right), \quad (15)$$

$$\frac{\partial \bar{\theta}}{\partial \tau} + Gr \bar{U} \frac{\partial \bar{\theta}}{\partial X} + Gr D\bar{\theta}\bar{V}$$

$$= \frac{1}{Pr} \nabla^2 \bar{\theta} + \frac{2S^2}{Pr} \left(X \frac{\partial \bar{\theta}}{\partial X} + YD\bar{\theta} \right) \quad (16)$$

subject to the boundary conditions

$$\bar{U} = \bar{V} = \bar{\theta} = 0 \quad \text{at} \quad Y = 0, 1. \quad (17)$$

In the above equations, $Gr =$ Grashof number function $f = 2(A - Y) + 3l(A - Y)^2$ where $A = (T_1 - T_m)/T_1$, and $\nabla^2 = (\partial^2/\partial X^2) + (\partial^2/\partial Y^2)$, with $\tau = \sqrt{dt/h^2}$ as dimensionless time (Fourier number).

A stream function $\hat{\psi}$ which satisfies the continuity equation (13) is defined as:

$$\bar{U} = D\hat{\psi}, \quad \bar{V} = -\frac{\partial \hat{\psi}}{\partial X}. \quad (18)$$

Introducing $\hat{\psi}$ into equations (13)–(17), eliminating the pressure \bar{P} by cross-differentiation and neglecting the terms containing the small parameter $(2S^2/Pr)$, the end result leads to:

$$\left(\frac{\partial}{\partial \tau} - \nabla^2 \right) \nabla^2 \hat{\psi} + Gr \frac{\partial}{\partial X} (\bar{U} \nabla^2 \hat{\psi} - D^2 \bar{U} \hat{\psi}) = D(f\bar{\theta}), \quad (19)$$

$$\left(\frac{\partial}{\partial \tau} - \frac{1}{Pr} \nabla^2 \right) \bar{\theta} + Gr \frac{\partial}{\partial X} (\bar{U} \bar{\theta} - D\bar{\theta} \hat{\psi}) = 0 \quad (20)$$

with the boundary conditions

$$\hat{\psi} = D\hat{\psi} = \bar{\theta} = 0. \quad (21)$$

In accordance with linear stability theory the formal solutions for the perturbations $\hat{\psi}$ and $\bar{\theta}$ may be taken in the form [6]

$$[\hat{\psi}, \bar{\theta}] = [\psi(\tau, Y), \theta(\tau, Y)] e^{iaX} \quad (22)$$

where a is the wave number of the disturbances, $i = \sqrt{-1}$. Substituting equation (22) into equations (18)–(21), one obtains the following eigenvalue problem:

$$\left[\frac{\partial}{\partial \tau} - (D^2 - a^2) \right] (D^2 - a^2) \psi + iaGr [\bar{U}(D^2 - a^2) \psi - D^2 \bar{U} \psi] = D(f\theta), \quad (23)$$

$$\left[\frac{\partial}{\partial \tau} - \frac{1}{Pr} (D^2 - a^2) \right] \theta + iaGr [\bar{U}\theta - D\bar{\theta}\psi] = 0, \quad (24)$$

$$\psi = D\psi = \theta = 0 \quad \text{at} \quad Y = 0, 1. \quad (25)$$

The above stability problem is solved by the application of the Galerkin method [16]. Following Ozisik and Hassab [17], the functions ψ and θ are represented by a series of orthogonal functions that satisfy the boundary conditions (25) as:

$$\psi(\tau, Y) = \sum_{m=1}^N d_m(\tau) \phi_m(Y), \quad (26)$$

$$\theta(\tau, Y) = \sum_{m=1}^N e_m(\tau) \psi_m(Y). \quad (27)$$

The orthogonal functions ϕ_m and θ_m are chosen as [18],

$$\phi_m(Y) = \frac{\cosh aY - \cos \mathcal{U}_m Y}{\cosh a - \cos \mathcal{U}_m} - \frac{\sinh aY - \mathcal{U}_m \sin \mathcal{U}_m Y}{\sinh a - \mathcal{U}_m \sin \mathcal{U}_m}, \quad (28)$$

$$\theta_m(Y) = \sin(m\pi Y) \quad (29)$$

and \mathcal{U}_m 's are the positive roots of

$$(\cosh a \cos \mathcal{U} - 1) + \frac{\mathcal{U}^2 - a^2}{2a\mathcal{U}} \sinh a \sin \mathcal{U} = 0 \quad (30)$$

The above solutions for ψ and θ are introduced into equations (23) and (24) and the orthogonality conditions are utilized to yield the following matrix equation:

$$\frac{d\mathbf{X}}{d\tau} + \mathbf{B}\mathbf{X} = 0 \quad (31)$$

where, $\mathbf{X} = \{d_m, e_m\}^T$ is the transpose of the coefficient vector associated with N -term expansion, and \mathbf{B} is a matrix of $2N \times 2N$ complex elements resulting from orthogonalization. The matrix eigenvalue problem (31) has a variable time coefficients because the Grashof number Gr is a function of the melting thickness h which is in turn a function of time $h = 2S\sqrt{\alpha t}$. However the rate of growth of this melting thickness is expected to be much smaller than that of the disturbance (ψ or θ). Therefore, it is quite reasonable to treat the coefficients of the matrix \mathbf{B} as constants in solving it with the complex QR algorithm [19, 20].

The stability criteria of this system is established by determining its eigenvalues $C_n = C_r + C_i$, (where C_i = wave speed, $n = 1, 2, \dots, 2N$). That is, for a given choice of the system parameter T_1 there is a least of two minimum values of Gr with respect to a that cause either the real part of the least eigenvalue $C_r = 0$, $C_i \neq 0$ for travelling waves, or both components $C_r = C_i = 0$ in the case of stationary cells. Below this value the heat flows by conduction only and the main flow is stable. Therefore, this minimum Grashof number corresponds to the onset of convection and is referred to as the critical Grashof number Gr_c . In carrying out the computations by the Galerkin method, for Pr based on the viscosity at the mean of the boundary temperatures, it is found that 10 terms in the series of trial functions are very sufficient to get an excellent convergence in the range of interest of T_1 . A sample of these results are illustrated in Table 1.

Table 1. Gr_c as a function of the number of approximation N

Data	N	4	6	8	10	12
$T_1 = 1^\circ\text{C}$ $a = 1.325$	Gr_c	456.75	420	476.5	480.23	481.25
$T_1 = 8^\circ\text{C}$ $a = 2.35$	Gr_c	3425	3271	3249	3247.3	3246.6

RESULTS AND DISCUSSION

The results of this analysis could be classified in terms of the stepped wall temperature T_1 into three regions of completely different characteristics: region I ($T_1 < 7.1^\circ\text{C}$), region II ($7.1 \leq T_1 \leq 9.4^\circ\text{C}$), and region III ($T_1 > 9.4^\circ\text{C}$). Before presenting the effect of each region on the onset of instability, it is important first, to consider the base flow velocity profile in these regions which will throw some light on this problem.

Figure 2(a) is a plot of the velocity profile in regions I

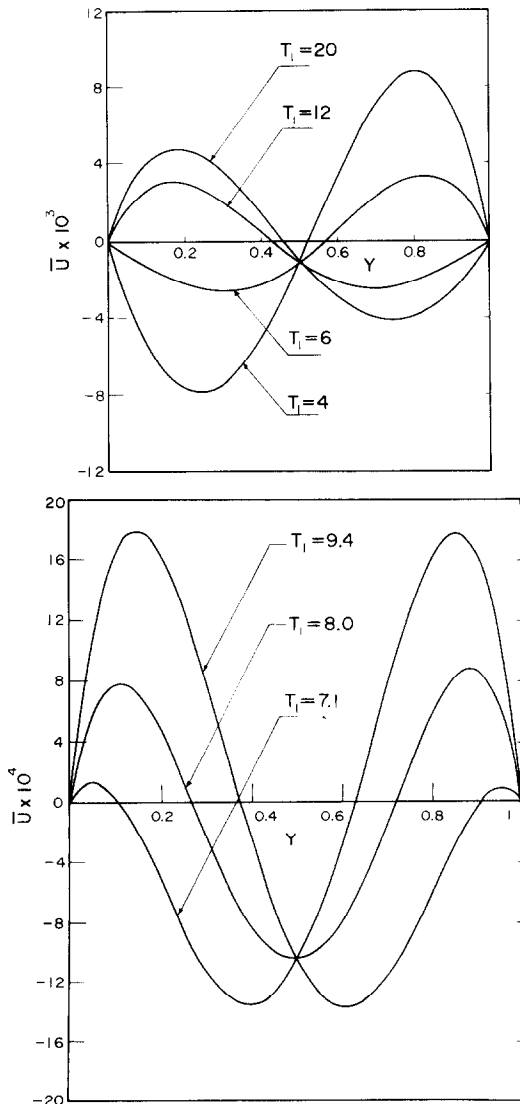


FIG. 2.

and III respectively. Clearly, in region I, a unicellular motion sets up in such a manner that the fluid near the hot wall descends down and that near the interface ascends upward. Conversely, in region III, an opposite unicellular motion occurs. The reason for this is that: In region I, the water layer near the hot wall is denser than that next to the interface, while in region III, the reverse is true. However, in region II, the fluid at the central part is denser than those next to the boundaries. Therefore, as it is shown in Fig. 2(b), two parallel cells set up, with the fluid at the central part moving downwards and those adjacent to the boundaries moving upwards. Furthermore, the effect of the stepped wall temperature T_1 on the base flow velocity \bar{U} could be explained with the help of Fig. 3, which is a plot of the average coefficient of thermal expansion $\bar{\beta}$ vs T_1 . When $T_1 < 8.2^\circ\text{C}$, $\bar{\beta}$ has a negative decreasing function, and for $T_1 > 8.2^\circ\text{C}$, $\bar{\beta}$ is positively increasing with T_1 . Since, the shear flow is driven by the buoyancy effects which are linearly dependent upon $\bar{\beta}$, so, increasing T_1 will suppress the non-dimensional base flow velocity in region I while expanding it in region III.

The solution of this problem for T_1 in the range from 1 to 30°C (i.e. $8 < Pr < 13.5$) indicates that the onset of instability sets in as oscillating waves travelling in the vertical direction with a wave speed, C_i , which is related to the maximum base flow velocity \bar{U}_{\max} as shown in Fig. 4. It is to be noted that, for water at room temperature or common fluids with $Pr < 12.7$, the onset of instability sets in as horizontal stationary cells [6]. The transition in the wave structure caused by the density anomaly of water could be due to the increasing participation of the potential energy associated with the perturbed buoyancy field on the disturbance energy, although this is still less than that generated from the base flow.

The calculations for the neutral stability curves summarized in Fig. 5 show that, as T_1 is increased, Gr_c increases in region I, has two peaks in region II at

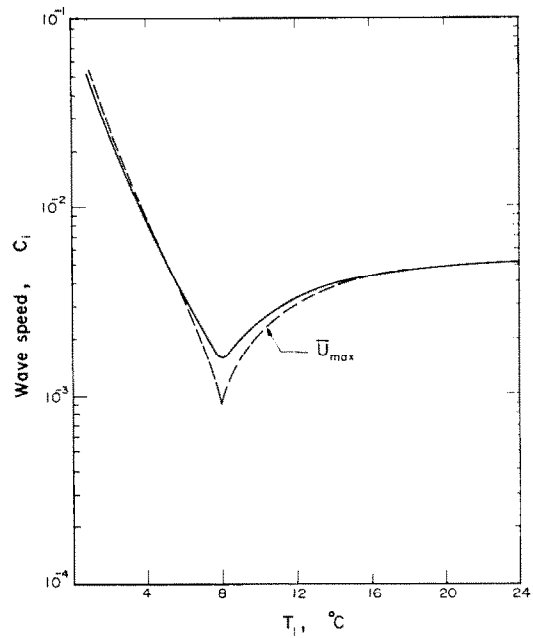


FIG. 4.

temperatures of 7.3 and 9.2°C respectively, and then gradually decreases in region III to a turning point at $T_1 = 15^\circ\text{C}$ where it increases again. The critical condition is also defined by another Grashof number \bar{Gr}_c based on the coefficient of thermal expansion β at the interface (absolute value), in order to compare the results with that for common fluids.

$$\bar{Gr} = \frac{\beta_0 g T_1 h^3}{v^2} \quad (32)$$

where β_0 is obtainable from equation (3) as

$$\beta_0 = \left. -\frac{1}{\rho_0} \frac{d\rho}{dT} \right|_{T=0} = (2\lambda_1 - 3\lambda_2 T_m) T_m \quad (33)$$

These two Grashof numbers are related by:

$$\bar{Gr} = 8.3965 \bar{Gr}/T_1 \quad (34)$$

In light of this relation, the modified critical Grashof number \bar{Gr}_c is calculated in terms of T_1 and presented with Gr_c in the same figure. As shown in the figure the curve of \bar{Gr}_c approaches an asymptotic value of about 1300 in region III.

The wave size at the critical condition expressed by the wave number a ($a = 2\pi/\Lambda$, Λ = wavelength) is found to vary with the stepped wall temperature T_1 reaching maximum value of $a = 2.34$ at $T_1 = 8^\circ\text{C}$ as shown in Fig. 6.

So far, in presenting the stability results for the critical Grashof numbers, we could not interpret the effect of heating on the stability of the flow; that is, at what values of T_1 , the instability is enhanced and/or delayed. The uncertainty is due to the dependence of Gr upon both T_1 and the melting thickness h which is not prescribable *a priori*. It is, therefore, appropriate to recast the stability results in terms of the melting thickness:

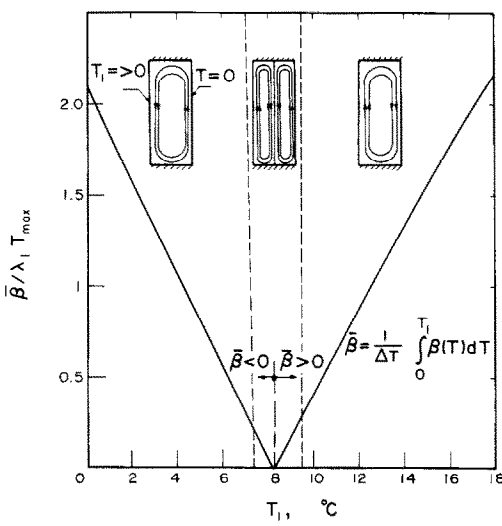


FIG. 3.

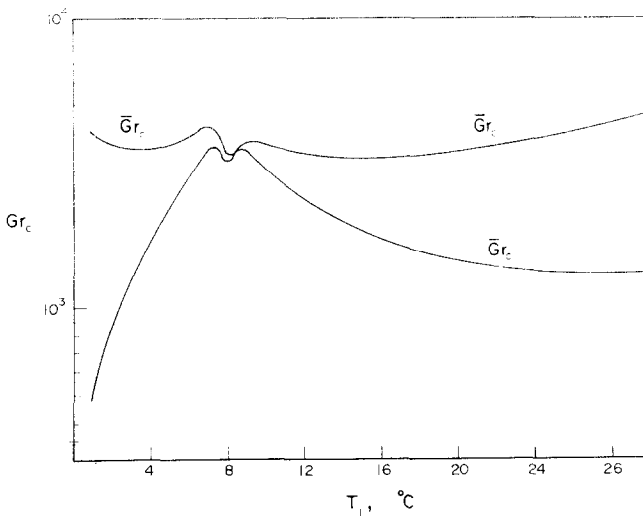


FIG. 5.

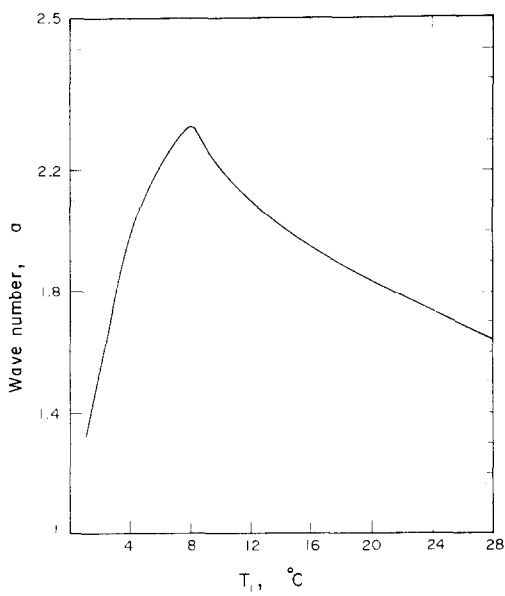


FIG. 6

has no maximum value, i.e. heating increases the density difference across the fluid layer, and accordingly, destabilizing the flow. When $T_1 > 4^\circ\text{C}$, the density profile has a maximum value due to the shift of the maximum density layer from the hot wall. In this case, heating has a smaller destabilizing rate although the instability sets in earlier owing to the higher temperature difference across the melted layer.

(2) In region II, an interesting but unexpected variation of h_c and t_c with the stepped wall temperature T_1 is noticed. This trend may be attributed to the transition in the wave structure from two-column waves for $T_1 < 7.1^\circ\text{C}$, to three-column waves for $7.1 \leq T_1 \leq 9.4^\circ\text{C}$, and back as two-column waves for $T_1 > 9.4^\circ\text{C}$.

(3) In region III, heating has a significant destabilizing effect because of the strong bending of the density profile resulting from the pronounced increase of the density difference.

SUMMARY AND CONCLUSIONS

The results of this problem which concerned with the stability of natural convection in a vertical melted ice layer initially at 0°C could be classified in terms of the stepped wall temperature T_1 into three regions:

(1) For $T_1 < 7.1^\circ\text{C}$, the instability sets in as two-column waves travelling oppositely in the vertical direction with a wave speed which is nearly equal to the maximum base flow velocity. As T_1 is increased, the wavelength increases to about 2.6 times the melting thickness h . Although heating increases Gr_c , it is actually destabilizing the flow with a decreasing rate.

(2) For $7.1 < T_1 < 9.4^\circ\text{C}$, the instability sets in as three-column waves. In this region, minimum wavelength and minimum wave speed occur at 8°C . Conversely, maximum values of Gr_c are observed at $T_1 = 7.3$ and 9.2°C respectively. In this region heating also

$$h_c = \left(\frac{Gr v^2}{\lambda_{1g} T_1^2} \right)^{1/3} \quad (35)$$

and the melting time:

$$t_c = \frac{h_c^2}{2S t_w x} \quad (36)$$

at the onset of instability as demonstrated in Fig. 7.

As shown in the Fig. 7, the effect of heating on the stability criteria expressed by h_c and t_c can be classified into three known regions as follows:

(1) In region I, when $T_1 < 4^\circ\text{C}$, the density profile

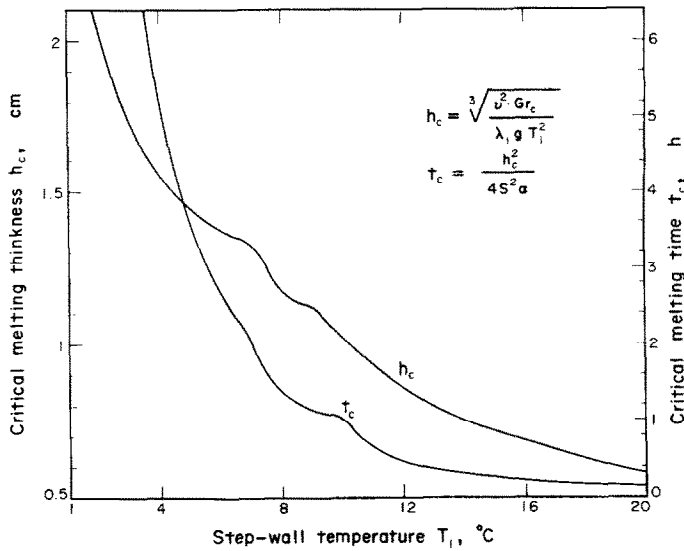


FIG. 7.

destabilize the flow.

(3) For $T_1 > 9.4^\circ\text{C}$, the instability sets back as two-column waves with both wave speed and wavelength increasing as T_1 is increased. Moreover, heating has a destabilizing effect on the flow.

REFERENCES

1. J. Straub, G. Meker, K. Küblbeck, A. Staudt and U. Grigull, Untersuchung der Konvektion in Jahrespeichern. *VDI-Berichte* **288**, 39–46 (1977).
2. G. Z. Gershuni, Stability of plane convective motion of a liquid, *Zh. Tech. Fiz.* **23**, 1838–1844 (1953).
3. R. N. Rudakov, Spectrum of perturbations of stability of convective motion between vertical planes, *P.M.M.*, **31**, 349–355 (1967).
4. C. M. Vest and V. S. Arpaci, Stability of natural convection in a vertical slot, *J. Fluid Mech.* **36**, 1–25 (1969).
5. A. E. Gill and C. C. Kirkham, A note on the stability of convection in a vertical slot, *J. Fluid Mech.* **42**, 125–127 (1970).
6. S. A. Korpela, D. Gözüm and C. B. Baxi, On the stability of the conduction regime in a vertical slot, *Int. J. Heat Mass Transfer* **16**, 1683–1690 (1973).
7. D. V. Boger and J. W. Westwater, Effect of buoyancy on the melting and freezing process. *J. Heat Transfer* **89**, 81–89 (1967).
8. Y. C. Yen, Onset of convection in a layer of water formed by melting ice from below, *Phys. Fluids* **11**, 1263–1270 (1967).
9. Y. C. Yen and F. Galea, Onset of convection in a water layer formed continuously by melting ice, *Phys Fluids* **12**, 509–516 (1969).
10. R. S. Tankin and R. Farhadieh, Effects of thermal convection currents on formation of ice, *Int. J. Heat Mass Transfer* **14**, 953–961 (1971).
11. R. S. Wu and K. C. Cheng, Maximum density effects on thermal instability by combined buoyancy and surface tension, *Int. J. Heat Mass Transfer* **19**, 559–565 (1976).
12. N. Seki, S. Fukusako and M. Sugawara, A criterion of onset of free convection in a horizontal melted water layer with free surface, *J. Heat Transfer* **99**, 92–98 (1977).
13. G. M. Merker, P. Waas and U. Grigull, Onset of convection in a horizontal water layer with maximum density effects, *Int. J. Heat Mass Transfer* **22**, 505–515 (1979).
14. Z. S. Sun, C. Tien and Y. C. Yen, Thermal instability of a horizontal layer of liquid with maximum density, *A.I.Ch. E. J.* **15**, 910–915 (1969).
15. E. M. Sparrow, L. Lee and N. Shamsundar, Convective instability in a melt layer heated from below, *J. Heat Transfer*, **98C**, 88–94 (1976).
16. B. A. Finlayson and L. E. Scriven, The method of weighted residuals and its relation to certain variational principles for the analysis of transport processes, *Chem. Engng Science*, **20**, 395–404 (1965).
17. M. N. Özisik and M. A. Hassab, Effects of convective boundary conditions on the stability of the conduction regime in an inclined slender slot, *Int. J. Num. Heat Transfer* **2**, 251–260 (1979).
18. C. L. Dolph and D. C. Lewis, On the application of infinite systems of ordinary differential equations to perturbations of plane Poiseuille flow, *Q. appl. Math.* **2**, 97–110 (1958).
19. P. C. Sukanek, C. A. Goldstein and R. L. Laurence, The stability of plane Couette flow with viscous heating, *J. Fluid Mech.* **57**, 651–670 (1973).
20. I. G. Choi and S. A. Korpela, Stability of the conduction regime of natural convection in a tall vertical annulus, *J. Fluid Mech.* **99**, 725–738 (1980).

APPARITION DE LA CONVECTION DANS UNE COUCHE DE GLACE EN FUSION ENTRE DES PLAQUES VERTICALES

Résumé—On étudie par une théorie linéaire la stabilité du régime de conduction de la convection naturelle dans une couche verticale de glace en fusion initialement à la température de fusion. Les courbes de stabilité, $Gr_c = Gr_c(T_1)$ et $h_c = h_c(T_1)$, montrent que le nombre de Grashof critique Gr_c et l'épaisseur critique fondue h_c sont dépendants de la température de la paroi T_1 et lorsque T_1 augmente le changement de mode transfert entre la conduction et la convection est accru pour toutes valeurs de T_1 dans le domaine 1–30°C. De plus l'instabilité apparaît en ondes se déplaçant verticalement, avec un écoulement secondaire avec des ondes à deux colonnes pour $T_1 < 7,1^\circ\text{C}$ et $T_1 > 9,4^\circ\text{C}$, et des ondes à trois colonnes pour $7,1^\circ\text{C} < T_1 < 9,4^\circ\text{C}$.

EINSETZEN DER KONVEKTION IN EINER SCHMELZENDEN EISCHICHT ZWISCHEN SENKRECHTEN PLATTEN

Zusammenfassung—Die Stabilität des Bereichs der Wärmeleitung der freien Konvektion in einer senkrechten schmelzenden Eisschicht wird unter der Annahme, daß sie zu Beginn die Schmelztemperatur habe, mit Hilfe der linearen Theorie untersucht. Die Stabilitätskurven $Gr_c = Gr_c(T_1)$ und $h_c = h_c(T_1)$ zeigen, daß die kritische Grashof-Zahl Gr_c und die kritische Schmelzdicke h_c von der sprungartig aufgebrachten Wandtemperatur T_1 in der Weise abhängig sind, daß mit steigendem T_1 die Änderung der Wärmeübergangsform von Leitung in Konvektion für alle Werte von T_1 im Bereich von 1 bis 30°C beschleunigt wird. Ferner wurde gefunden, daß die Instabilität in Form senkrecht wandernder Wellen einsetzt, wobei die Sekundärströmung für $T_1 < 7,1^\circ\text{C}$ und $T_1 > 9,4^\circ\text{C}$ als Zweisäulen-Welle und für $7,1^\circ\text{C} < T_1 < 9,4^\circ\text{C}$ als Dreisäulen-Welle erscheint.

ВОЗНИКНОВЕНИЕ КОНВЕКЦИИ ПРИ ПЛАВЛЕНИИ СЛОЯ ЛЬДА МЕЖДУ ВЕРТИКАЛЬНЫМИ ПЛАСТИНАМИ

Аннотация — С помощью линейной теории исследуется устойчивость режима теплопроводности при естественной конвекции в вертикальном слое льда при его плавлении. Предполагается, что вначале слой находится при температуре плавления. Кривые устойчивости $Gr_c = Gr_c(T_1)$ и $h_c = h_c(T_1)$ показывают, что критическое число Грасгофа Gr_c и критическая толщина зоны расплава h_c зависят от температуры стенки T_1 : по мере увеличения T_1 переход от режима теплопроводности к конвекции усиливается при всех значениях T_1 , лежащих в диапазоне от 1 до 30°C. Кроме того найдено, что неустойчивость возникает в виде вертикальных бегущих волн, причем при $T_1 < 7,1^\circ\text{C}$ и $T_1 > 9,4^\circ\text{C}$ вторичное течение состоит из двухрядных волн, а при $7,1^\circ\text{C} < T_1 < 9,4^\circ\text{C}$ — из трехрядных волн.